

## RESULTS OF THE SLAC LCLS GUN HIGH-POWER RF TESTS\*

D. H. Dowell<sup>#</sup>, E. Jongewaard, C. Limborg-Deprey, J. Schmerge,  
Z. Li, L. Xiao, J. Wang, J. Lewandowski, A. Vlieks  
SLAC, Menlo Park, CA 94025, U.S.A.

### Abstract

The beam quality and operational requirements for the Linac Coherent Light Source (LCLS) currently being constructed at SLAC are exceptional, requiring the design of a new RF photocathode gun for the electron source. Based on operational experience at SLAC's GTF and SDL and ATF at BNL as well as other laboratories, the 1.6cell s-band (2856MHz) gun was chosen to be the best electron source for the LCLS, however a significant re-design was necessary to achieve the challenging parameters. Detailed 3-D analysis and design was used to produce near-perfect rotationally symmetric rf fields to achieve the emittance requirement. In addition, the thermo-mechanical design allows the gun to operate at 120Hz and a 140MV/m cathode field, or to an average power dissipation of 4kW. Both average and pulsed heating issues are addressed in the LCLS gun design. The first LCLS gun is now fabricated and has been operated with high-power RF. The results of these high-power tests are presented and discussed.

### DESCRIPTION OF THE LCLS GUN

The LCLS RF photocathode gun is a descendant of the BNL/SLAC/UCLA s-band gun whose design has been optimized to allow operation at higher repetition rate (120Hz) and improved quality of the RF fields[1,2]. The new features incorporated into the LCLS gun are:

1. Dual RF feed to eliminate phase asymmetry and dipole fields
2. Racetrack shaped full cell to correct for RF quadrupole fields
3. Increased 0-pi mode separation from 3.5 to 15MHz to reduce mode-beating and improve field quality
4. Shaped intervening cell iris to reduce field 10% below cathode field.
5. Z-couple to the waveguide to reduce pulsed heating
6. Deformation tuners rather than slug tuners.
7. Cooling designed for 120Hz, 140MV/m operation.

The interior surfaces of the LCLS gun is shown in Figure 1 where the z-coupling ports and the racetrack shape are easily seen. The gun design and measured parameters are given in Table I. The gun meets all the physics design requirements.

In addition the focusing solenoid has been built with both dipole and quadrupole magnetic field correctors. The solenoid fields were fully characterized using hall probe and rotating coil measurements.

\* Work supported by US DOE contract DE-AC02-76SF00515.

<sup>#</sup> dowell@SLAC.Stanford.edu

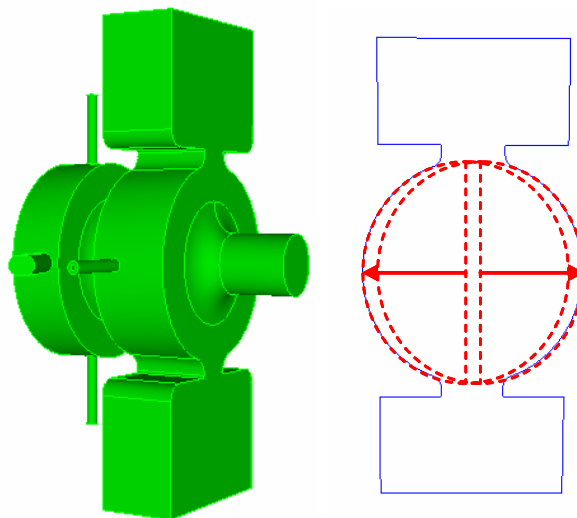


Figure 1: Interior surfaces of the LCLS RF photocathode gun.

Table I: LCLS gun parameters.

<i>RF Parameters</i>	<i>Design</i>	<i>Measured</i>
$f_{\pi}$ (GHz)	2.855987	2.855999
$Q0$	13960	13900
$\beta$	2.1	2.03
<i>Mode Sep. <math>\Delta f</math> (MHz)</i>	15	15.17
<i>Full Cell to Half Cell Field Ratio</i>	1	1

### RF COLD TEST RESULTS

The gun tuning and cells field ratio was studied as a function of mode separation to both equalize the field in both cells and to establish the method for changing cathodes. The ratio of cell fields vs. mode separation is given in Figure 2.

The final assembly of the gun with its solenoid is shown Figure 3. The view is from the cathode side of the gun to illustrate the dual RF feed extending to the right above and below the gun cathode flange. The waveguide splits again into two RF windows before being combined into a single waveguide back to the klystron.

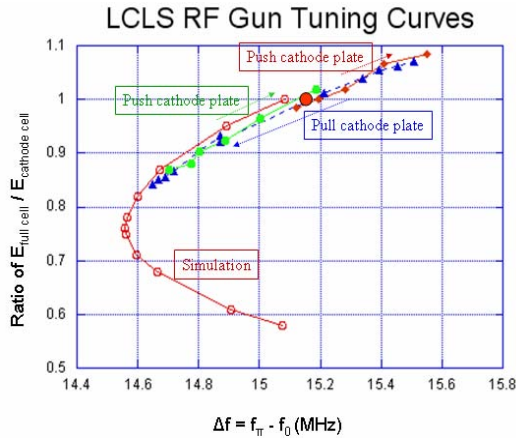


Figure 2: Full cell to half cell (cathode cell) field ratio as a function of 0-pi mode separation.

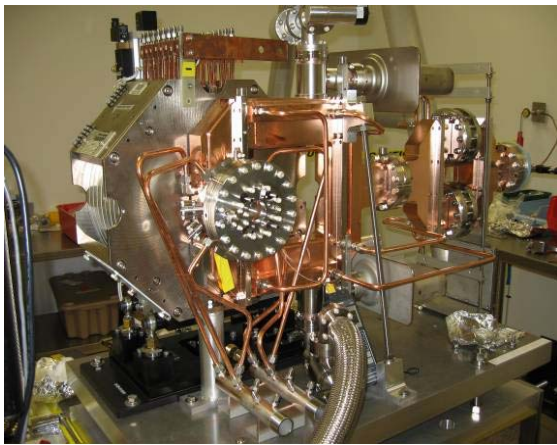


Figure 3: Gun1 and solenoid assembly in the SLAC vacuum lab.

### HIGH POWER RF TEST RESULTS

The gun was tested at full power in the SLAC Klystron Lab using the High-power RF circuit shown in Figure 4. There was no active temperature control of the gun body temperature. Therefore the resonance frequency would vary over a period of minutes to hours depending upon the average power dissipation, water temperature variation and other effects. The RF source frequency was manually adjusted to match the resonant frequency drifts and maintain the coupling into the gun and minimize the reflection.

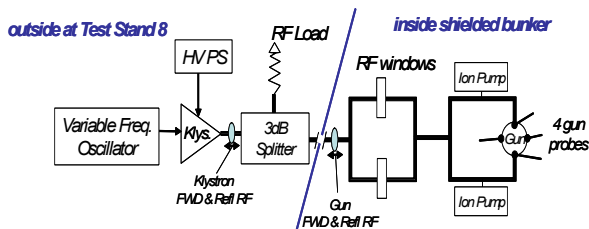


Figure 4: Configuration of the RF system used during conditioning of the LCLS RF gun.

### RF Conditioning

The gun was conditioned over a period of three weeks beginning Oct and ending Nov, 2006. A typical processing curve to high field is given in Figure 5, where the cathode field and the dark charge per RF pulse is plotted vs. time. The RF pulse was approximately 2 microseconds long as shown in Figure 6.

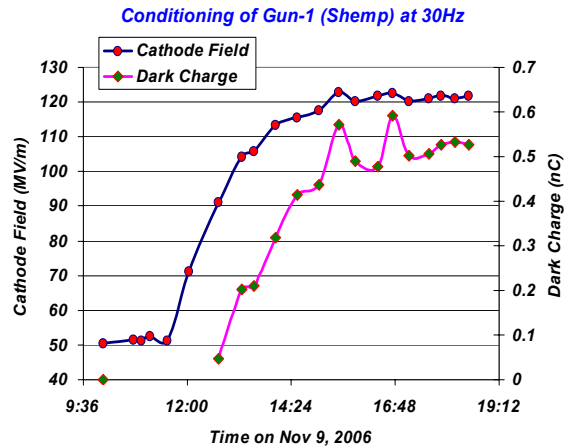


Figure 5: The cathode field and dark charge while conditioning to high power.

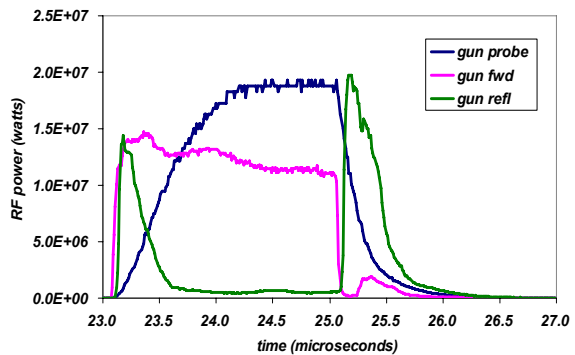


Figure 6: The RF power as measured using a peak power analyzer using calibrations for probes, couplers and cables. See Figure 4 for the location of measurements in RF circuit.

The observed scaling of dark charge with cathode field is plotted in Figure 7. This is the same data as in Figure 5 and exhibits a quadratic behavior.

The dark charge was also imaged using a 100 micron thick YAG crystal placed in front of the Faraday cup. The surface of the Faraday cup was polished and served as a 45 degree mirror to reflect the YAG image out a vacuum window for viewing with a digital camera. The gun solenoid was adjusted to study the dark charge and to maximize charge collection in the Faraday cup. A typical image is seen in Figure 8. A detailed analysis is given in a companion paper to these proceedings [3].

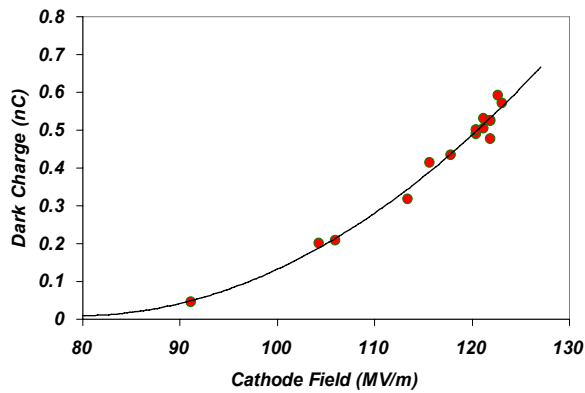


Figure 7: Dark charge vs. the peak cathode field.

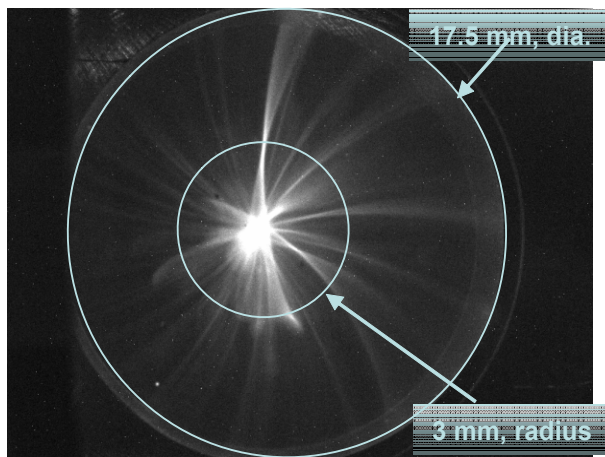


Figure 8: Image of dark charge on a 100 micron thick YAG crystal scintillator.

The faraday signal is plotted with one of the gun RF probes in Figure 9. The fast oscillation at the beginning of the waveforms is HV modulator noise.

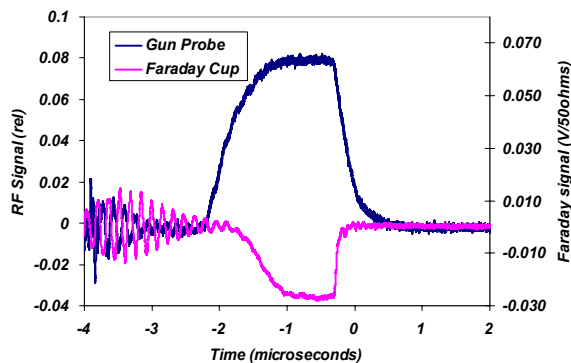


Figure 9: Gun probe and the faraday cup signals.

### Imaging the Cathode Surface

The condition of the cathode surface was determined by visual inspection through the grazing incidence ports. A typical image is shown in Figure 10. The depth of focus

is small due to the 70 degree viewing angle, and clearly shows a damage spot due to an arc during commissioning. Beam measurements performed after the gun was installed and operated at Sector 20 show this mark is offset from the gun axis and has little effect on beam performance.

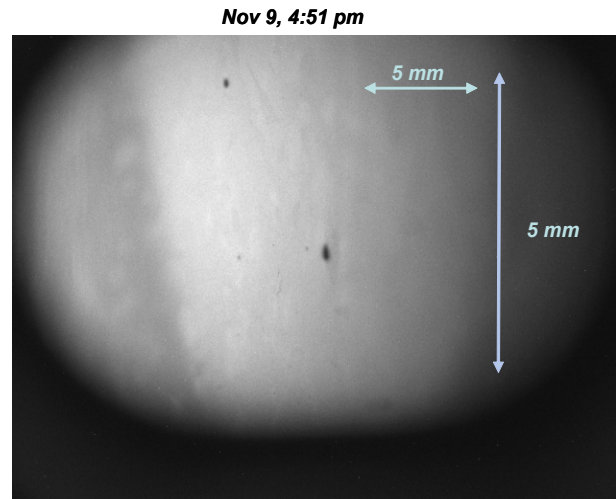


Figure 10: White light image of the cathode area as viewed and illuminated through the grazing-incidence laser ports.

### Gun Probe Thermal Measurements

It was observed that the gun probe calibrations increased with average power as a result of being heated by the RF fields and currents. Analysis determined that although the probe coupling was only -55db, there was still wall current heating in the probe tips. As a result this heating limits Gun1 operation at Sector 20 to a conservative 30Hz and 115MV/m. The probes have since been redesigned to have weaker coupling ( $\sim$ -75db) and constructed of copper-plated stainless steel. The new probes have been installed in Gun2 and will be tested in its high power tests. Gun1 probes will be upgraded to the new design in the future.

### REFERENCES

- [1] C. Limborg-Deprey, D. Dowell, J. Schmerge, Z. Li and L. Xiao, "RF Design of the LCLS Gun" LCLS-TN-05-3, Feb. 2005.
- [2] L. Xiao, R.F. Boyce, D.H. Dowell, Z. Li, C. Limborg-Deprey, and J.F. Schmerge, "Dual Feed RF Gun Design for the LCLS", SLAC-PUB-11213.
- [3] D.H. Dowell, E. Jongewaard, C. Limborg-Deprey, J. Schmerge and A. Vliks, "Measurement and Analysis of Field Emission Electrons in the LCLS Gun," These Proceedings.